Annals of Agricultural Science, Moshtohor (ASSJM)
https://assjm.journals.ekb.eg/
www.fagr.bu.edu.eg
© 2023, Faculty of Agriculture, Benha University, Egypt. ISSN:1110-0419
Original Article Vol. 61(4) (2023), 781 –796 DOI: 10.21608/assjm.2024.250610.1256

Impact of Irradiated or Non-Irradiated Nanomaterials on Decontamination of Pb and Cd in Wastewater

E.A. Shehab[2], H.M. Salem[1], S.M. Soliman[2], Y.G.M. Galal[2] and M.A. Abdel-Salam[1]
[1]Soil and water, Faculty of Agriculture, Benha University.
[2] Nuclear Research Center Soil and Water Research Department, Egyptian Atomic Energy Authority, Abou-Zaabal, 13759, Egypt.

Abstract

Chemically synthesized nano zeolite and nano-rice char were prepared to be used as adsorbents for Pb and Cd from the artificially contaminated water. Properties and elemental configuration of nanoparticles were identified. X-ray Diffraction (XRD) and Fourier Transform Infrared Spectroscopy (FT-IR) were utilized to identify the functional groups accountable for the sorption of the concerned contaminants by the nanoparticles. The hydroxyl group was identified as the peak detected in the FT-IR analysis of nano zeolite, whereas the bands of rice straw char were attributed to several broad peak functional groups, including hydroxyl groups and others. These nanoparticles' activities were investigated at various values of the nano sorbent mass and temperature. Increasing the nano sorbent mass from 0.25 to 0.75 g, a significant improvement in removal efficiency of the elements under study. however, beyond, 0.75 g of the nano biosorbent mass did not significantly alter the sorption process. Given that a temperature rise improves the interaction between the sorbent and the metal ions, the findings revealed that the high mobility of metal ions may also be responsible for the increase in metal ions sorption by the Nano sorbent. Furthermore, in comparison with the non-irradiated sorbents, the irradiated ones showed a decreased capability for removing Pb and Cd. The correlation coefficient (R2) values for both Pb (II) and Cd (II) ions indicate that Langmuir's model succeeded in description of sorption of both Pb indicating that adsorption is the main process responsible for Pb and Cd sorption by the nano sorbents under study. The maximum adsorption capacity (qmax) values for Pb (II) and Cd (II) ions were determined to be 4.09 mg/g and 7.18 mg/g, respectively, based on the Langmuir model. These findings indicated that, because of the habitation of active sites, the values of the constant K2 for the biosorbent materials exposed to gamma radiation were greater than the corresponding ones of the nonirradiated nano sorbent materials.

Key words: Adsorbents, Adsorption isotherm, Cd, Pb, Irradiation, kinetics, Nanomaterials, Rice char, Wastewater, Zeolite

Introduction

Water is essential for all life on the planet. Despite covering 71% of the earth's total area, only 3% of the water is freshwater and less than 1% is drinkable. The remaining percentage of water is inaccessible in various forms such as ice, glaciers, and snow at the southern and northern poles **(Kabir, et al. 2019**). Various pollutants present in wastewater, including heavy metals, turn out to be the most common contaminants in contaminated water, deteriorating environmental sustainability. One such way that potentially hazardous components enter the food chain is through the irrigation by wastewater. Heavy metal pollution in water has adversely affected human health worldwide due to the rapid development of industries, economies, and populations (**Hasanpour and Hatami, 2020**)., Alleviation of such contaminants became a necessity. Sorption is considered as one of the most efficient processes used for removing water contaminants (**Ali et al. 2016**; **Ahmad et al. 2020**), whereas it has no generated secondary wastes (**Mthomben et al. 2016**).

Recently, biochar as an effective amendment was widely used for decontamination of polluted wastewater or soil (**Azadi and Raiesi 2021; Luo et al. 2022; Wang et al. 2021**), and successfully eliminated contaminants from wastewater, lowering its soil bioavailability (**Sun et al. 2022**). (**Li et al. 2020; Lian et al. 2020; Ren et al. 2022; Zhang et al. 2019**). In this regard, nano biochar differs greatly from bulk biochar in that it has a significantly greater specific surface area (SSA), a smaller hydrodynamic radius, a higher negative zeta potential, and a greater number of functional groups that contain oxygen. (**Lyu et al. 2018; Naghdi et al. 2017; Pratap et al.**

2022; Ramanayaka et al. 2020b). Previously, **Li et al. (2017); Yue et al. (2019); and Vishnu et al. (2022)** deduced that nano biochar could strongly sorb Cd, Pb or Cu in aqueous system, and the heavy metal removal rate increases gradually as the concentration of nano biochar increases and They attributed that to adsorbent exchangeable sites and the larger SSA of nano biochar. Nano biochar could adsorb pollutants via complex mechanisms including ion exchange, complexation, precipitation, electrostatic interaction, and physical adsorption (**Zhang et al. 2022**). In this regard, the interaction between the negatively charge surface carrying oxygen-containing functional groups as electron donors and positively charged metals was found as the main mechanism responsible for the adsorption of heavy metals by nano biochar **(Jia et al., 2022**). Otherwise, the complexation of the positively charged –OH groups of nano biochar with the negatively charged Cr (VI) in aqueous systems was detected as the dominant mechanism involved in the adsorption process **(Wang et al. 2020**).

Perfect performance of nano biochar in environmental remediation was strongly affected by pH, coexisting ions, dissolved organic matter (DOM), organisms and root exudates (soil system) (**Jiang et al., 2023**). Low pH levels allow the functional groups of nano biochar to readily protonate to create H^+, which will reduce the adsorption capacity of nano biochar by creating a competition between H^+ and cation pollutant species for cation adsorption sites (**Mahmoud et al. 2020; Park et al. 2019**). Furthermore, because of electrostatic repulsion, positively charged surfaces may prevent contaminants from adhering to them. (**Lyu et al. 2018**). In various studies, it has been observed that the ability of nano biochar to adsorb Cd increases as the pH level rises within the range of 1 to 7 (**Mahmoud et al. 2021; Ramanayaka et al. 2020a**). This phenomenon is likely linked to the protonation of the nano biochar surface during acidic adsorption, facilitating Cd in displacing H+ for adsorption sites. Nevertheless, it is noteworthy that the negatively charged nano biochar surface exhibits reduced affinity for negatively charged or neutral pollutants at elevated pH levels, primarily due to electrostatic repulsion (**Zeng et al. 2019**). Similar findings have been reported in earlier researches, indicating that the adsorption capability of nano biochar rises with an increase in pH within the range of 2 to 8, tapering off gradually beyond a pH of 8 (**Li et al. 2020; Sun et al. 2022**).

Utilization of biochar along with burned rice husk ash (RHA) that has a large surface area, light in weight, extremely porous in nature made an excellent adsorbent to deal with the mobility of deadly metals in the polluted soils (**Bhattacharyya et al. 2020**), showed great results regarding the soil health and its interaction with metals (**Zama et al. 2018).** In this respect, the presence of functional groups like phosphate, amino, carboxyl, sulfhydryl, phenol and amide assist biosorbents to form complexes with heavy metals and kick them out of the contaminated soils (**Singh et al. 2019**).

Zeolite is a naturally occurring crystalline aluminosilicate that may be produced artificially in regulated circumstances. It is found in sedimentary rocks. Over the recent decades, natural zeolite, and surface-modified zeolites (SMZs) have gained recognition as eco-friendly materials with diverse applications. They are used in, wastewater treatment, and serve as adsorbents for remediation purposes (**Younas et al., 2023**). Both natural and synthetic zeolites demonstrate promise in wastewater remediation, excelling not only in the removal of chromaticity and turbidity but also in the mitigation and detoxification of heavy metal cations and ammonium .and other organic contaminants like xylene, benzene, and others. Nonetheless, it is well known that utilizing natural zeolite may effectively eliminate cations like phosphate and oxyanions of heavy metals (**Syafalni, et al., 2014**). When eliminating divalent cadmium ions from wastewater using microwave-treated zeolites, **Fahmy et al. (2016**) found that the best duration for doing so was 140 minutes using 0.25 g of zeolite in 25 mL of wastewater polluted with cadmium. Another method of physical modification is the use of ultrasonic waves in which sound waves of different frequencies and strength increased the adsorption capacity. As reviewed by **Tahoon et al., (2020),** the use of the modified clinoptilolite zeolite nanoparticles offered an excellent elimination of cadmium pollutants from water with adsorption capacity of 138.9 mg/g.

Cadmium ion chelation took place through both ion exchange with raw clinoptilolite zeolite nanoparticles and complexation with the functional groups of pentadic acid. This underscores the significant contribution of functionalization in augmenting the adsorption capacity. The adsorption process occurred through monolayer and multilayered adsorption (**Al Sadat Shafiof and Nezamzadeh-Ejhieh 2020**).

Based on the previous literature, this work aimed at characterization of synthesized nanoparticles of zeolite and rice straw char and following up its potential in removing Cd and Pb from the artificial contaminated water as affected by environmental factors, i.e. temperature, and sorbent mass.

Materials and Methods

Rice straw as field waste and zeolite (It is a mineral like clay minerals) were selected and prepared as nanomaterials to be used as sorbent for Pb and Cd from the artificially contaminated water. Preparation and characterization of such materials were carried out as following:

Preparation of Rice straw char (RS)

Rice straw residues were collected from the experimental farm of Soil & Water Research Department, Nuclear Research Center, Atomic Energy Authority, Inshas, Egypt, as low-cost agricultural leftovers. To eliminate dust and other soluble pollutants, RS samples were repeatedly rinsed with tap water and subsequently with distilled water. They were then allowed to dry for 48 hours in a greenhouse under the sun. Next, a mechanical grinder was used to grind the dry rice straw into a fine powder. For one hour, rice straw was burned at 300 °C in a muffle furnace.

Preparation of zeolite:

The nano-sized was prepared by using a ball mill to grind zeolite for six hours, until it was of the nano scale and the particle size was determined using XRD.

(ICP-OES) Inductively coupled plasma optical emission spectroscopy Prodigy High Dispersion ICP, Leeman, USA, was used to determine the initial and final concentrations of Pb and Cd in solution.

Characterization of the prepared nano sorbents

FT-IR characterization

Fourier transform infrared spectroscopy (FTIR) uses the infrared portion of the electromagnetic spectrum. The infrared range has a shorter frequency and a longer wavelength than the visible range. The scanning range is set at 4000 to 400 cm^{-1} while the spectral resolution is 4 cm^{-1}. The bonds between different elements absorb infrared radiation at different frequencies, which is the basis for FTIR analysis. The compositions of the various synthetic sorbents (rice straw Char and zeolite) was analyzed for their vibrational spectra using a Fourier transform infrared spectrometer and a simulation instrument. NICOLET iS10 image in the scan area 4000-400 cm^{-1} as potassium bromide. In this case, the sample was thoroughly mixed with KBr (1:10% by mass). The resulting substrate was ground and compressed into a disk 5.0 mm in diameter and 1.0 mm thick. The infrared spectrum is scanned over the wavelength range of 4000-400 cm^{-1}.

X- Ray Diffraction (XRD)

The particle sizes of tested materials determination (nm)

The technique of X-ray diffraction (XRD) was employed to study the sizes present in the tested nano sorbents by examining their diffraction patterns. The particle size can be estimated from the width of the diffraction peaks using the **Scherrer equation**:

$$B\ (2\theta) = k\ \lambda\ /\ D\cdot \cos\theta$$

$$\mathbf{D}=\frac{0.94\times\lambda}{\beta\cos\theta}$$

where D is the average crystallite size perpendicular to the reflecting planes, λ is the x-ray wavelength, θ is the Bragg angle, β is the width of the peak in radians due to the finite size of the crystal, and the numerical constant K is a function of the crystallite shape but is generally taken as being about 1.0 for spherical particles. The shape factor has a typical value of about 0.9, but varies with the actual shape of the crystallite; but for which Scherrer (1918) obtained the value $2/\pi)^{½}$ =0. 93 but Patterson, (1939), modified the shape factor (k) by the value = 1.107∼ 1.11.

Using equations (1) and (2), the sorption capacity of the sorbent qe (mg g^{-1}) and the removal efficiency of Pb (II) and Cd (II) (R %) were determined.

The removal efficiency of either of Pb or Cd (R%) and the adsorbent Qe (mg g^{-1}) may be calculated using equations (1) and (2).

$$R\ \% = \frac{(Co-Ce)}{Co}\times 100 \qquad (1)$$

The adsorption capacity was calculated using following equation 2;

$$Qe\ (mg/g) = \frac{(Co-Ce)}{M}\times V \qquad (2)$$

Effect of sorbent mass

The effect of sorbent mass on the removal (sorption) of Pb (II) and Cd (II) ions from aqueous solution was determined at the optimum pH of 6 for Pb (II) and Cd (II) ions. A 50 mg/L of either Pb (II) Cd (II) ion solution was mixed with different masses (0.25, 0.50 and 0.75 g) of either rice straw char or nano Zeolite. These suspensions were then stirred using a mechanical shaker at 200 rpm and 25°C for 60 min. After the set time, the sample mixture was then removed from the mechanical stirrer and allowed to stand for 60 min. The sample mixture was then filtered with Whatman filter paper 42 and the amount of metal ions remaining was determined using an ICP. The analysis of Pb (II) and Cd (II) ions at different sorbent mass values was carried in triplicate.

Effects of temperature

The effect of temperature on the sorption of Cd^{2+}, and $Pb^{2+}$was investigated at 25°C, 35°C, and 45°C equivalent to 298 °F, 308 °F and 318 °F with an absorbent dose of 0.50 g and an initial concentration of 50 mgL^{-1} for both the two tested elements. These studies were conducted at a pH of 6 with a contact time of 30 min to ensure that equilibrium was achieved. The sample mixtures were then stirred using a mechanical shaker at 200 rpm and after that they were filtered with Whatman filter paper No. 42. Pb (II) and Cd (II) ions in the equilibrium solutions at each of the studied temperatures equilibrium were

determined using an ICP. All analyzes performed at the concerned different temperatures were carried out in triplicate.

Sorption isotherm:

Sorption is commonly characterized using isotherms, which express the quantity of adsorbate on the sorbent relative to its concentration at a constant temperature. Normalizing the adsorbed quantity by the mass of the adsorbent enables the comparison of adsorption isotherms for various materials. In this context, Langmuir, Freundlich, and Temkin models were applied to analyze the experimental data of equilibrium.

Langmuir Isotherm:

The Langmuir isotherm is based on assuming a monolayer sorption that homogeneity distribute onto a surface sorbent active site and is given by the following linear equation (Langmuir 1918).

$$\frac{Ce}{qe} = \frac{1}{qmaxK} + \frac{Ce}{q\,max}$$

Where, K is the Langmuir constant ($L \cdot mg^{-1}$) related to the apparent energy of sorption, q_{max} is the quantity of adsorbate required to form a single monolayer per unit mass of sorbent ($mg \cdot g^{-1}$), considered as the maximum sorption capacity and q_e is the amount adsorbed on unit mass of the sorbent ($mg \cdot g^{-1}$) when the equilibrium concentration is Ce ($mg \cdot L^{-1}$).

Freundlich Isotherm:

The Freundlich sorption isotherm is an empirical equation interprets the multilayer sorption on heterogeneous sorbent active sites and is being expressed by this linear equation (Freundlich, 1907).

$$\log qe = \log kf + \frac{1}{n} \log Ce$$

where qe is the amount of solute sorbed per unit mass of sorbent(mg/g) and the equilibrium solute concentration in the bulk solution is Ce (mg/L). According to **Tran (2022)**, 1/n represents the strength of the adsorption process, and KF (mg/g) is the isotherm constant.

Temkin Isotherm:

The Temkin isotherm, which may be expressed by the following equation in its linearized version (**Temkin 1940**), was used to assess the level of sorption temperature and bonding energies of the molecules in layer during sorbate and sorbent interactions.

$$q_e = B \ln A + B \ln C_e$$

Where qe (mg/g) and Ce (mg/L) represent the amount of solute sorbed per unit mass of sorption and the equilibrium solute concentration in the bulk solution, respectively. Plotting qe against the natural logarithm of Ce allows for the determination of A and B.

Result and Discussion

Nano-crystalline size of both rice char and zeolite was determined using X-ray diffraction method recording 35.66 and 13.74 nm, respectively (**Table 1**). The XRD pattern indicates that the rice straw char and zeolite had shown a cubic structure.

Table 1. XRD pattern of the nano crystallite size rice straw char and zeolite.

Tested Materials	D	I/Io	2θ	θ deg	θ Rad	β FWHM (deg)	*β Rad*	Crystallite size (nm)
Rice char	3.151	100	28.3036	14.1518	0.2470	0.2297	0.004009	35.6671
Zeolite	3.932	100	22.5956	11.2978	0.1972	0.5906	0.010297	13.7416

Characterization of rice straw char by FT-IR

FT -IR of 0.75 g non-treated char (Fig.1), those treated at 40 °C temperature whether non-irradiated or irradiated with 20 kGy dose, (Fig.2) and the corresponding ones at 45 c^0 (Fig.3) show many bands were seen from the FTIR several functional groups with wide peaks, such as hydroxyl groups at (3754-3737 cm^{-1} and (3436-3450 cm^{-1}). According to **Alhamdi et al. (2019)**, rice straw exhibited an intense and wide spectrum within the 3100–3500 cm^{-1} region, suggesting the presence of a hydrogen-bonded (–O–H) functional group in cellulose. According to **AlHumaidan, et al. (2022)**, the assignment carbon related chemical (C-H) stretching bands aliphatic chains at (2940 – 2917 cm^{-1}).

It was found that there are many additional peaks in these spectra at the longer wavelength region (1500 – 400) cm^{-1}. Although it is generally difficult to select specific functional group identifications in this region, it still contains valuable information. The results show that N–O asymmetry extends from the band at 1475 cm^{-1}. Then, the presence of a broad peak at ~1106 cm^{-1} indicates the stretching vibration of Si–OH. The presence of Si-O and CH_3 at functional groups of 802 cm^{-1} on the FTIR spectra may potentially increase the Cd adsorption on the coal surface **(Liang et al.,2022**). In addition to the bands at 785 cm^{-1} aromatic C-H, C=O and C=C stretching vibrations can be generated **Jing. et al.,2022)**. The FTIR of straw char seems to have sorption peaks at the (675-690) cm^{-1} range related to Fe-O bonding **(Rather et al., 2023**). The FTIR results are consistent with the XRD analysis results. All the functional groups recorded on the FTIR spectra of the prepared rice char in this

research were like those reported previously with different biomass derived chars (**Jia et al.,2023**). The presence of functional groups on the surfaces of rice straw derived chairs provides binding sites for ions, inducing their potential as sorbents for different pollutants from aqueous solutions.

These results are in consistent with those of **Yin et al. (2022)**, because the presence of multiple functional groups on the biochar surface can provide the highest coordination affinity for heavy metals. In an aqueous solution, protons from these functional groups of rice straw biochar exchange with Cd ions. Consequently, on modified biochar, several surface functional groups like COO^{-}, CH_2, and OH may increase the surface negatively of the biochar. The coordination affinity of COO^{-} and O^{-} for H^{+} may have contributed to the decrease in negative charge of biochar as the pH decreased and the zeta potential of biochar samples became less negative. These findings are consistent with those of **Baral et al. (2020)** who suggested that the sorption of heavy metals on the surface of BC can release H^{+} ions, leading to a decrease in solution pH, especially at higher metal concentrations and greater sorption capacity during the sorption study.

Char control

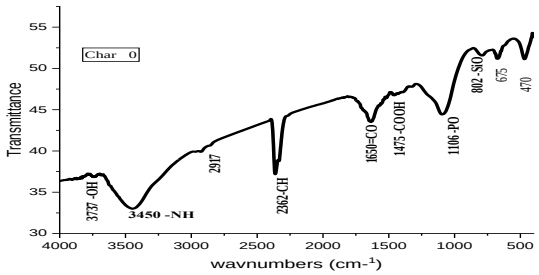

Fig. 1: FTIR spectra of the rice straw char as sorbent material without any treatments.

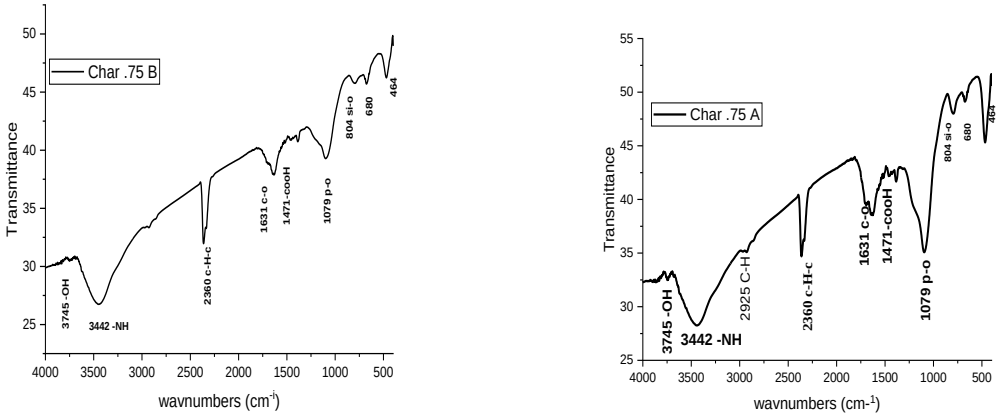

Fig. 2: FTIR spectra of the rice straw char as sorbent material at of 0.75 g under a temperature of 40 c^0 0.75 g non-irradiated a and irradiated with gamma ray at a dose 20 kGy b.

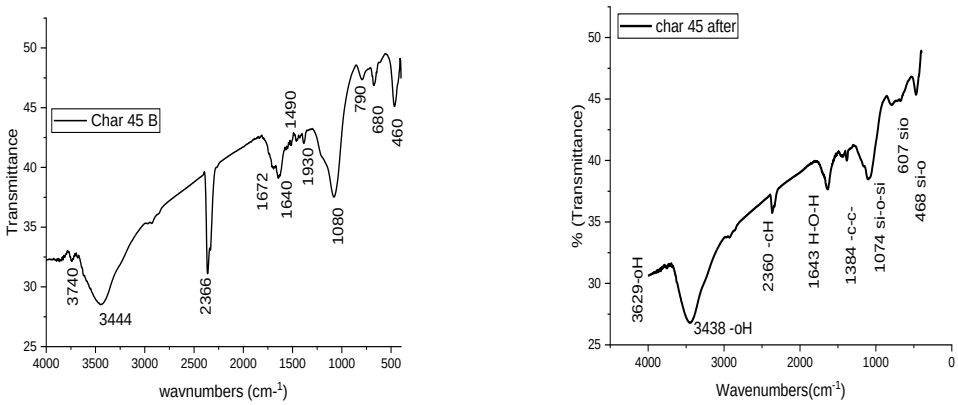

Fig. 3: FT-IR spectra of the rice straw char as a sorbent material after under a temperature of 45 °C, non-irradiated (a)and irradiated with gamma ray at a dose of 20 kGy (b).

Characterization of zeolite by FT-IR

FT-IR spectra of zeolite are shown in **Figs. (4 - 6)**. The detectable peaks observed at a wavelength ranging from 3865 – 3428 cm^{-1} are attributed to OH^- stretching of water molecules in the zeolite caves in control after loading with lead or cadmium on a sorbent mass of 0.75 g, at 45°C.

Al. Sofy, (2018) analyzed the FTIR spectra of 13-X zeolite (Si/Al=1.75) before any treatment and before adsorption of ammonia. She found different Si-OH-Al band at 3474cm^{-1} which can be Brønsted acid sites. **Baral et al., (2020)** explained that increasing the exchange degree resulted in increases in the intensities of the Si-OH-Al band and resulted in a shift of the band from 3464 to 3441 cm^{-1}. The intensity of OH band depends on the concentration of OH as well as the extinction coefficient of OH band. The band at (1637-1633) cm^{-1} ascribed to H_2O. The deformation mode arises due to the incomplete dehydration of the synthetic zeolite, indicating the presence of unbound water within the zeolite structure. The structure of zeolite should be considered as a set of interconnected (TiO_4) units (SiO_4) and (AlO_4) tetrahedral). The most intense absorption bands of silicates are found within specific wavenumber ranges. (1200–1060) cm^{-1} (asymmetric stretching vibrations Si–O–Si and Si–O–Al) and 550–400 cm−1 (bending vibrations O–Si–O). In the control treatment, at the band~ 800 cm^{-1} which shifted to 670 cm^{-1} regions after loading with lead or cadmium a sorbent mass of 0.75 g, at 45°C and at contact time up to 3h, these bands are corresponding to the symmetrical stretching vibrations Si–O– (Si, Al). The band at about 570 cm^{-1} seems to be the most sensitive to cation exchange. As can be concluded from the spectrum (the band at about 466 cm^{-1}), the intensity of this band is the highest for the ion with the largest radius (in the case of the analyzed experiment using XRD, these are K^+ and Na^+ ions).

Additionally, the characteristic bands associated with the asymmetric stretch mode (973.24 cm^{-1}), symmetric stretch mode (666.08 cm^{-1}), double six-member rings (D6R, 561.21 cm^{-1}) and a bending mode of the T-O bond (460.11 cm^{-1}), are observed (where T is Al or Si). The spectra data are consent with lithium slag-based zeolite X (**Ke, et al, 2019**).

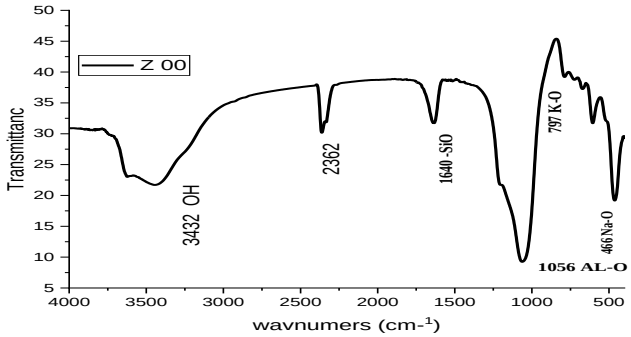

Fig. 4: FTIR spectra of zeolite as a sorbent without any treatments.

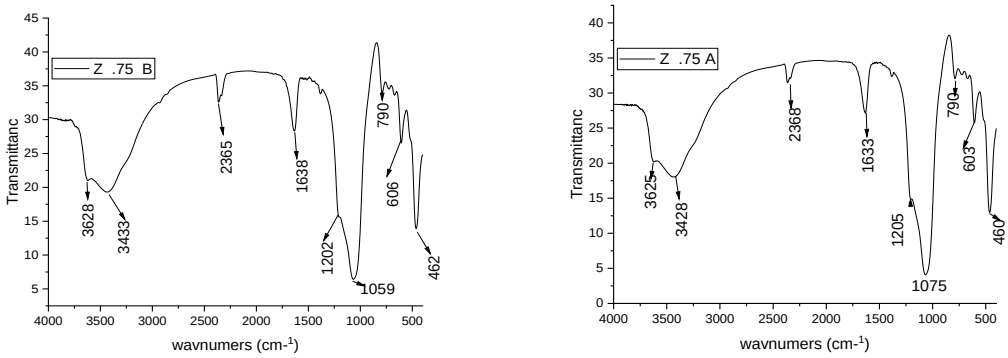

Fig. 5: FTIR spectra of zeolite as a sorbent of 0.75 (g) mass, a) non-irradiated and b) irradiated with gamma ray at a dose of 20 kGy.

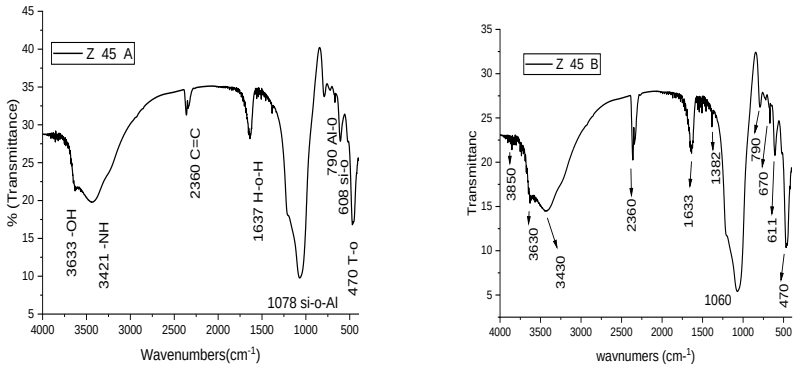

Fig. 6: FTIR spectra of zeolite as a sorbent after exposure to 45 °C temp., a) non-irradiated and b) irradiated with gamma ray at a dose of 20 kGy.

Effect of sorbent Mass

Sorption was tried under mass various amounts of sorbent ranging from 0. 25 to 0.75 g at an initial cadmium and lead concentrations of 50 mg/L, a pH value of 6 for 60 minutes at a constant room temperature (25°C) g. Table (2) and Figure (7) show that the ability to sorb or remove lead and cadmium increased rapidly as the amount of zeolite or char derived from rice straw increased, due to the increase in available surface area with increasing their amounts . Therefore, removal efficiency increased significantly when the mass of sorbent was increased from 0.25 to 0.75g. Increasing mass of the sorbent beyond this level did not cause further significant change in the sorbed amount of either Pb or Cd. These results agree with those of **(Deng et al., 2019).** On the other hand, the sorbed amount of either of the considered metal ions per unit mass of the adsorbent decreased with increasing mass of the sorbent.

Table 2. Effects of sorbent (mass irradiated and non-irradiated) on sorption capacity of Cd and Pb (mg g^{-1})

Nano Materials	Adsorbent dose (g)	Pb		Cd	
		Non-irradiated	Irradiated	Non-irradiated	Irradiated
Rice Char	**0.25**	5.99	6.32	5.60	5.20
	0.50	4.57	4.94	4.22	4.11
	0.75	3.13	3.38	2.87	2.83
	Mean	**4.56**	**4.88**	**4.23**	**4.05**
Zeolite	**0.25**	6.30	6.90	6.24	5.87
	0.50	4.61	4.97	4.34	4.21
	0.75	3.13	3.38	2.92	2.87
	Mean	**4.68**	**5.08**	**4.50**	**4.32**

This probably occurred du to one of two factors: During the sorption process, increasing the amount of sorbent in a fixed volume and concentration leads the adsorption sites to become saturated. Secondly, increased sorbent mass may cause particle interactions through particle accumulation, which could result in decreased sorption capacity. As a result, the ideal sorbent concentration for use in later trials was determined to be 50 mgL^{-1} in 50 mL of the aqueous solution.

According to the findings of **(Shamsollahi and Partovinia 2019)**, the sorption capacity of the rice husk controls the percentage of metal sorption within a specific range of initial metal concentration**.** the sorption capacity of the rice husk controls the percentage of metal sorption within a specific range of initial metal concentration The sorption capacity of Pb and Cd by different sorbents tended to decrease with increasing sorbent mass but was not significantly impacted by irradiation (Table 2). The highest removal of lead and cadmium was obtained at the sorbent mass of 0.75 g. There was not much difference between the sorbent sources whether they were irradiated or not.

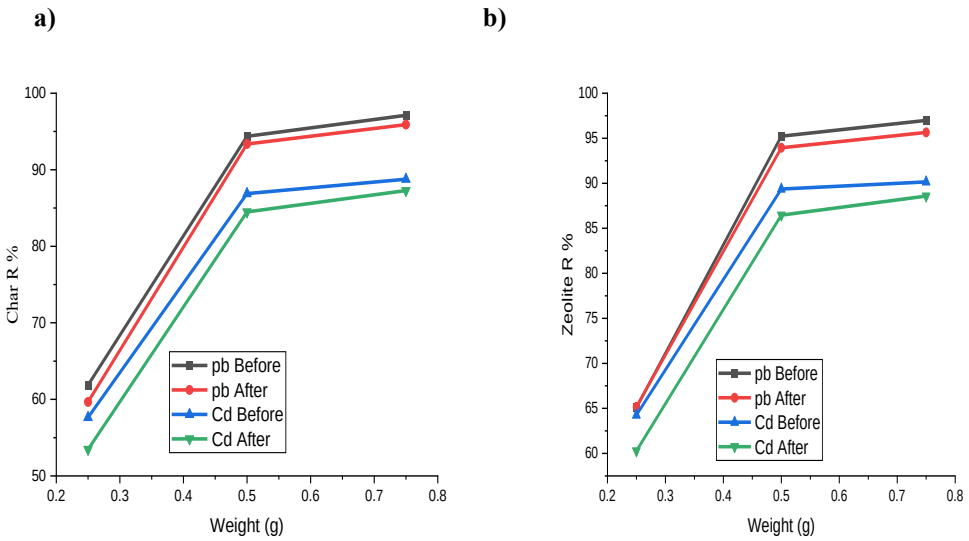

Fig. 7: Effects of Adsorbent Mass on removal efficiency (%) of Cd and Pb (mg g^{-1}) from artificial wastewater using a) nano-char and b) nano-zeolite as adsorbed materials either non-irradiated or irradiated with gamma ray.

Effect of temperature

The highest removal of Pb and Cd from the artificially contaminated waters (or their corresponding sorption by char and zeolite) was attained at 45°C. The percentage of lead and cadmium removal effectiveness on straw char and zeolite was investigated as a function of temperature. The experiments were conducted at 25, 35, and 45 °C (298, 308, and 318 °k) with a starting lead and cadmium content of 50 mg/L, a constant 0.5 g sorbent mass, and a pH of 6. The findings demonstrate that as temperature rises, sorption increases and so does the removal efficiency (%) (Table 3).

The high mobility of metal ions may be responsible for the increase in metal ion removal since a rise in temperature increases the contact surfaces between the sorbent and ions,. This suggests that all tested sorbents undergo endothermic sorption of lead or cadmium. (**Shang et al., 2019**). A temperature of 45°C was selected for additional studies

Table 3. Effects of temperature (°F) on removal efficiency (%) of Cd and Pb from artificial wastewater using selected irradiated and non-irradiated adsorbed materials.

Adsorbent Materials	Temperature (°F)	Pb		Cd	
		Non-irradiated	Irradiated	Non-irradiated	Irradiated
Rice Char	**298 °F**	89.73	84.81	81.95	81.01
	308 °F	92.99	87.85	88.54	84.48
	318 °F	96.98	88.97	90.61	86.53
Mean		**93.23**	**87.21**	**87.03**	**84.01**
Zeolite	**298 °F**	91.15	87.	84.22	81.94
	308 °F	93.42	88.74	92.45	84.68
	318 °F	97.10	91.20	93.47	88.24
Mean		**93.89**	**89.18**	**90.05**	**84.95**

Table 4. Effects of temperature (°k) on sorption Capacity (Qe) of Cd and Pb (mg g-^{1}) from artificial wastewater using irradiated and non-irradiated sorbents.

Sorbent Materials	Temperature (°F)	Pb		Cd	
		Non-irradiated	Irradiated	Non-irradiated	Irradiated
Char	**298 °F**	4.63	4.37	3.95	3.94
	308 °F	4.80	4.53	4.27	4.11
	318 °F	5.00	4.59	4.37	4.21
Mean		**4.81**	**4.50**	**4.20**	**4.09**
Zeolite	**298 °F**	4.70	4.52	4.06	3.99
	308 °F	4.82	4.58	4.46	4.12
	318 °F	5.01	4.70	4.50	4.30
Mean		**4.84**	**4.60**	**4.34**	**4.14**

due to the higher sorption occurred at this temperature compared with the other the temperatures under study. The equilibrium value of sorption capacity of Pb and Cd on straw nano-char, and nano-zeolite, was found to extend with temperature increment of 25°C (298°F) to 45°C (318°F) (**Table 4**). The increment in sorption capacity was 4.63 to 5.00; and from 4.7 to 5.01 mg/g for Pb on the above materials, respectively. However, for Cd sorption capacity, it increased from 3.95 to 4.37 and from 4.06 to 4.50 mg/g for the previous treatments, respectively, demonstrating that lead and cadmium ions are sorbed on the sorbent preferentially at higher temperatures. The retention of both elements is endothermic. At high temperature, the ions are easily dehydrated and thus their sorption capacity becomes more favorable. When the sorbents were irradiated with 20 KGy dose of gamma the sorption capacity values for both lead and Cd diminished.

Sorption equilibrium isotherms

Plotting the concentration of the considered element at equilibrium (Ce) against values of Ce/qmax was found to fit the linear form of Langmuir model, as seen in Figure (8).

Langmuir's model works well with both lead and cadmium metal ions. The correlation coefficients for Pb (II) and Cd (II) ions were found to be 0. 9978 and 09983, which means the model fits the data very closely. According to the Langmuir model, the most chemicals that can be sorbed for Pb (II) is 4. 09 mg/g and for Cd (II) is 7. 18 mg/g. The value (kl) for the reaction of Pb (II) ion is 0. 3576 and for Cd (II) ion is 0. 0763, showing a favorable reaction (**Qu. Et al, 2020**).

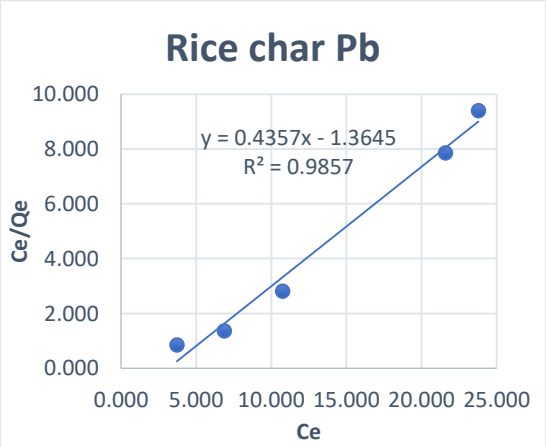

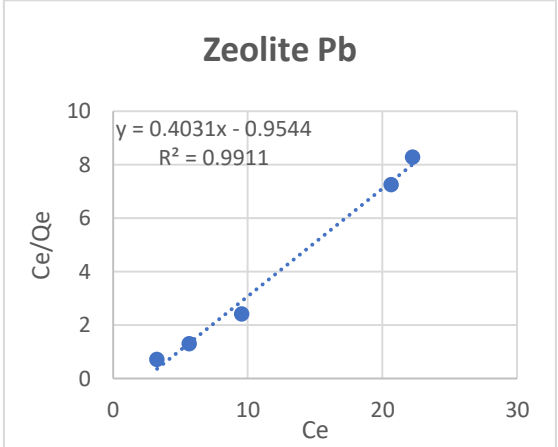

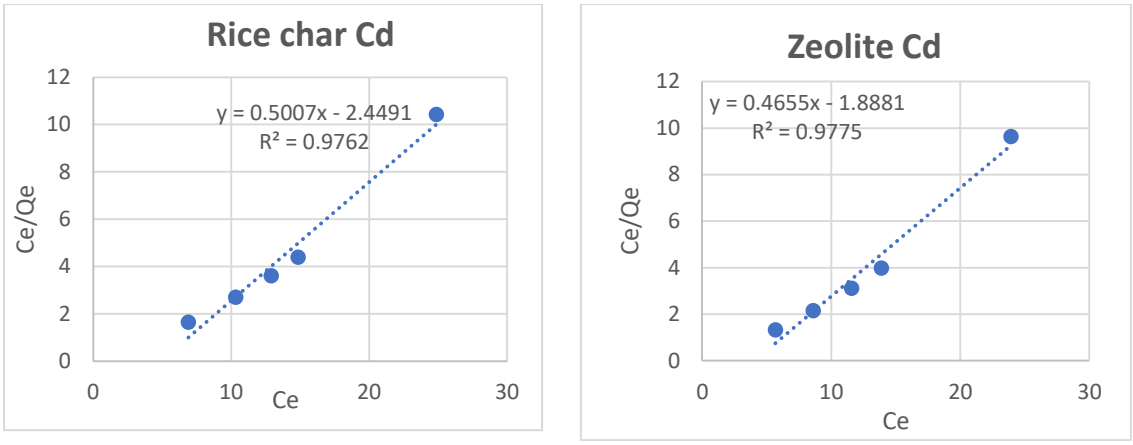

Figure 8. Equilibrium sorption using Langmuir isotherm constants for the sorption capacity (qe) of lead and cadmium ions from wastewater onto nanoparticles of rice char and zeolite.

Table (5) shows that he Langmuir model was able to show that the sorption data had very good correlation with R2 values >0. 9702.

For the Freundlich model (Table 5 and Fig. 9), the two metals reflected good correlation coefficients. The correlation coefficient (R^2) values for Pb (II) ion were 0.9111 and 0.9121 when using nano-char and nano-zeolite, respectively. In case of Cd (II), the R2 values were 0.9157 and 0.9070 for the same sequence. It means that both nano-char and nano zeolite were nearly closed to each other in case of Pb sorption while nano-char was more effective in sorbing Cd comparable to nano zeolite .

Table 5. Calculated equilibrium sorption Langmuir, Freundlich and Temkin isotherm constants for the sorption capacity of lead and cadmium ions from artificial contaminated wastewater.

Nanoparticles	Langmuir			Freundlich			Temkin		
	K_L	b	R2	K_F	b	R2	K_T	b	R^2
					Pb				
Rice char	**0.7329**	**-3.1317**	**0.9857**	**9.8425**	**0.1568**	**0.9111**	**0.0038**	**-2223.03**	**0.9578**
Zeolite	**2.4807**	**-0.4224**	**0.9911**	**1.5806**	**4.6115**	**0.9121**	**0.0028**	**-2420.45**	**0.9507**
					Cd				
Rice char	**0.4083**	**-4.8914**	**0.9762**	**0.9834**	**-2.3281**	**0.9157**	**0.0065**	**-1764.78**	**0.9548**
Zeolite	**0.5296**	**-4.0561**	**0.9775**	**1.0541**	**-2.5038**	**0.9070**	**0.0051**	**-1960.88**	**0.9469**

Previous research conducted by **Afroze et al., (2016)** revealed that the overall adsorption capacity (K_F) for Pb (II) and Cd (II) ions was 0.3677 and 1.6339, respectively. The n-value of Pb (II) ion is 1,594 and that of Cd (II) ion is 1.672, demonstrating favorable and heterogeneous sorption reaction of Pb (II) and Cd (II) ions on activated carbon. The value of the regression coefficient R2 for Jovanovic model for two metal ions is 0.7172 for Pb (II) ion and 0.9351 for Cd (II) ion which is very weak, so it does not describe the adsorption well of two metal ions on activated carbon.

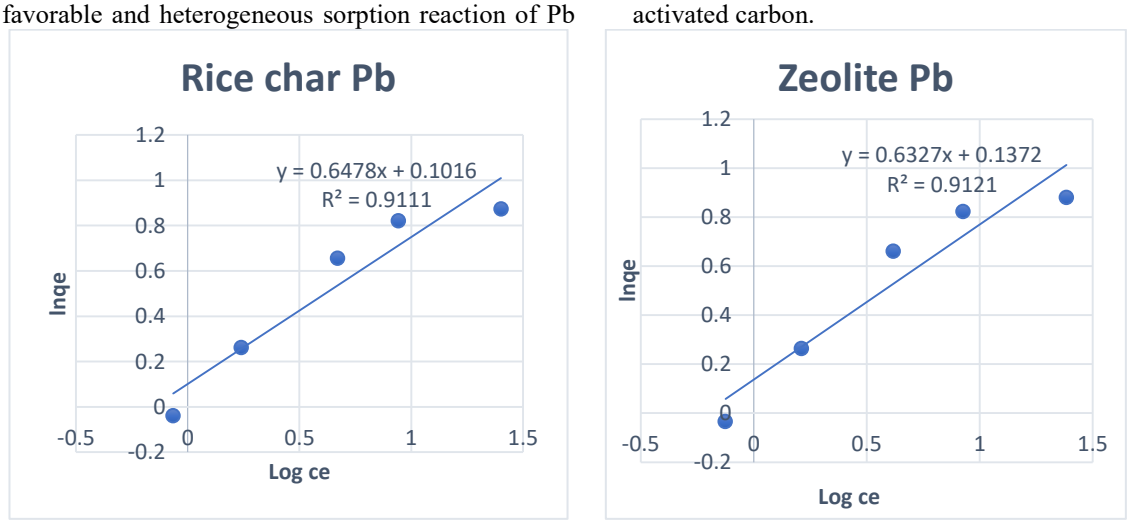

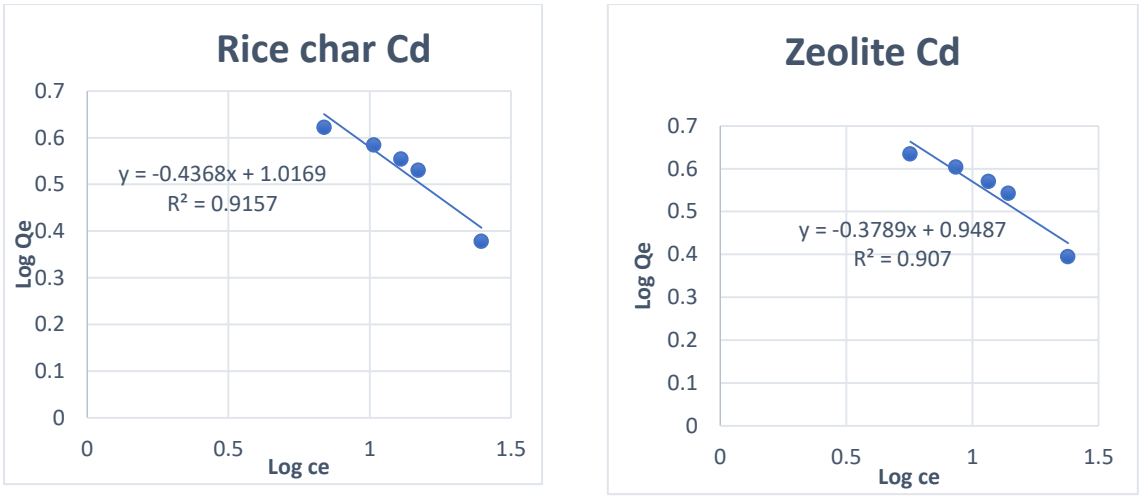

Figure (9). Equilibrium sorption using Freundlich isotherm constants for the sorption capacity (qe) of lead and cadmium ions from wastewater onto nanoparticles of rice char and zeolite.

The regression coefficient values for the Temkin model show that there were no significant differences between nano char and nano zeolite in adsorption of both metals. The obtained values of the correlation coefficient are 0.9578 for nano char > 0.9507 of nano zeolite for Pb (II) ion and 0.9548 0.9548 for nano char > 0.9469 of nano zeolite, for Cd (II) ions.

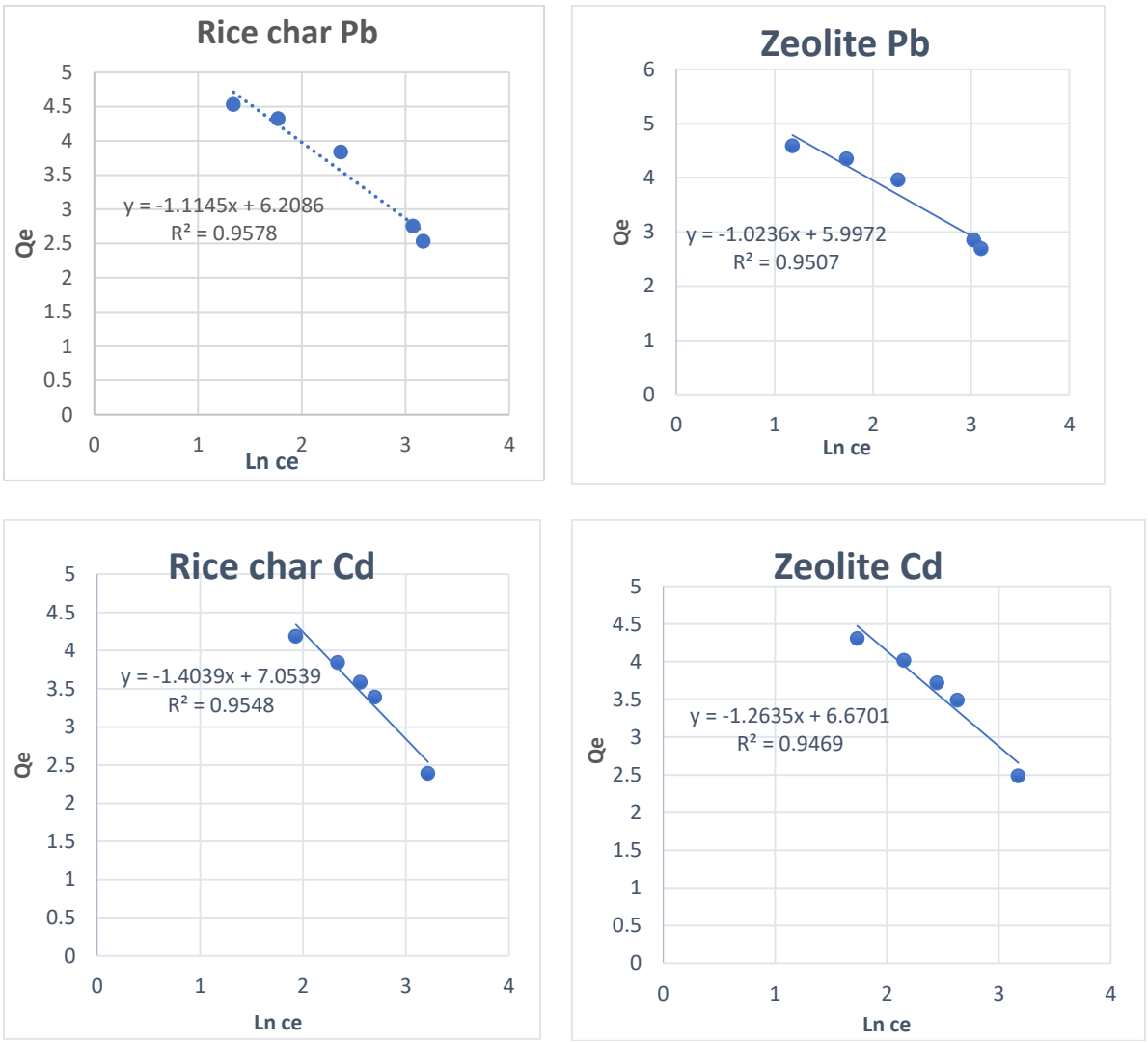

Figure 10. Equilibrium sorption using Temkin isotherm constants for the adsorption capacity (qe) of lead and cadmium ions from wastewater onto nanoparticles of rice char and zeolite.

In accordance, **Younes et al., (2019)** indicated that their data were found to fit Langmuir model well, comparable to Freundlich model, with the regression coefficient (R_2) of 0.99 and total adsorption capacity (qmax) of 158 mg/g; which is so close to the experimental value (145 mg/g). They added that obedience of the experimental data to Langmuir adsorption isotherm model reflects that the binding sites on the surface of corn cobs-nZVI adsorbent are homogeneously distributed and the total observed adsorption capacity was obtained due to a monolayer adsorption of Cd (II) ion on the surface of the adsorbent. Recently, **Singh et al., (2023)** examined two isotherm models, viz., The Freundlich adsorption isotherm and the Langmuir adsorption isotherm were examined, and it was noted that the Langmuir adsorption isotherm was best fitted to the experimental data of lead and cadmium. Therefore, they only considered the Langmuir adsorption isotherm in their study.

Conclusion

This work revealed that rice straw char and zeolite materials prepared in nanoscale have a potential for adsorbing Pb and Cd from the contaminated aqueous media. The characterization methods proved that these nanomaterials have different function groups and wide specific surface area that responsible for enhancing removal of Pb and Cd. Both removal percentages and adsorption capacity of both metals were adversely affected by increasing the adsorbent concentrations in liquid media (contaminated wastewater). These values were not significantly affected by irradiation where values of non-irradiated and irradiated nanomaterials nearly close to each other. Contrary, the increase of temperature up to 318 °F caused gradual increases in removable Pb and Cd percentages. Similar trend was noticed with adsorption capacity of both metals. On the other hand, the irradiation treatment has no significant effect on removal percent and adsorption capacity as affected by temperature Adsorption equilibrium isotherms of Cd and Pb removed by nano-rice char and nano-zeolite indicated fit Langmuir model well, comparable to Freundlich and Temkin models, with the regression coefficient (R_2) of 0.99.

References

Afroze, Sharmeen & Sen, Tushar & Ang, Ha. (2016). Adsorption removal of Zinc (II) from Aqueous Phase by Raw and Base Modified Eucalyptus Sheathiana Bark: kinetics, mechanism, and equilibrium study. Process Safety and Environmental Protection. 102. 10.1016/j.psep.2016.04.009.

Al Sadat Shafiof, M.; Nezamzadeh-Ejhieh, A. A (2020). Comprehensive study on the removal of Cd (II) from aqueous solution on a novel pentetic acid-clinoptilolite nanoparticles adsorbent: Experimental design, kinetic and thermodynamic aspects. Solid State Sci. 99, 106071

Al. Sofy Shatha Abd-Alhameed, (2018). Fourier Transformation Infrared Spectroscopic Studies of Acidity of NaH-13 X Zeolites. Al-Nahrain Journal for Engineering Sciences (NJES) Vol.21 No.3, pp.428-435. http://doi.org/10.29194/NJES.21030428

AlHumaidan, F. S., Rana, M. S., Vinoba, M., Rajasekaran, N., AlHenyyan, H. Y., and Ali, A. A. (2022). Synthesizing few-layer carbon materials from asphaltene by thermal treatment. *Diamond and Related Materials*, *129*, 109316.

Azadi N, Raiesi F (2021) Biochar alleviates metal toxicity and improves microbial community functions in a soil co-contaminated with cadmium and lead. Biochar 3:485-498

Baral, K., Li, A., and Ching, W. Y. (2020). Ab initio study of hydrolysis effects in single and ion-exchanged alkali aluminosilicate glasses. *The Journal of Physical Chemistry B*, *124*(38), 8418-8433.

Chen H, Gao Y, Li J, Sun C, Sarkar B, Bhatnagar A, Bolan N, Yang X, Meng J, Liu Z, Hou H, Wong JWC, Hou D, Chen W, Wang H (2022) Insights into simultaneous adsorption and oxidation of antimonite [Sb(III)] by crawish shell-derived biochar: Spectroscopic investigation and theoretical calculations. Biochar 4:37

Deng, Y., Huang, S., Laird, D. A., Wang, X., and Meng, Z. (2019). Adsorption behaviour and mechanisms of cadmium and nickel on rice straw biochars in single-and binary-metal systems. *Chemosphere*, *218*, 308-318.

Fahmy, A., Youssef, H., Elzaref, A. (2016). Adsorption of cadmium ions onto zeolite-A prepared from Egyptian kaolin using microwave. Int. J. Sci. Res. 5, 1549–1555.

Freundlich HMF (1906) Over the Adsorption in Solution. J Phys Chem 57:385–471

Hasanpour, M.; Hatami, M. 2020. Photocatalytic performance of aerogels for organic dyes removal from wastewaters: Review study. J. Mol. Liq., 309, 113094. [CrossRef]

Jia, Y., Zhang, Z., Li, M., Ji, N., Qin, Y., Wang, Y., and Sun, Q. (2022). The effect of hydroxypropyl starch on the improvement of mechanical and cooking properties of rice

noodles. *Food Research International*, *162*, 111922.

Jing, Y., Shakouri, M., Liu, X., Hu, Y., Guo, Y., and Wang, Y. (2022). Breaking C─ C Bonds and Preserving C─ O Bonds in Aromatic Plastics and Lignin via a Reversing Bond Energy Cleavage Strategy. *ACS Catalysis*, *12*(17), 10690-10699.

Kabir, S.; Cueto, R.; Balamurugan, S.; Romeo, L.D.; Kuttruff, J.T.; Marx, B.D.; Negulescu, I.I. 2019. Removal of acid dyes from textile wastewaters using fish scales by absorption process. Clean Technol. 1, 311–324. [CrossRef]

Ke, G., Shen, H., and Yang, P. (2019). Synthesis of X-Zeolite from waste basalt powder and its influencing factors and synthesis mechanism. *Materials*, *12*(23), 3895.

Langmuir I (1918) The adsorption of gases in plane surfaces of glass, mica and platinum. J Am Chem Soc 40:1361–1403

Li, B., Liu, D., Lin, D., Xie, X., Wang, S., Xu, H., Wang, J., Huang, Y., Zhang, S. and Hu, X., 2020. Changes in biochar functional groups and its reactivity after volatile–char interactions during biomass pyrolysis. *Energy & Fuels*, *34*(11), pp.14291-14299.

Lian F, Yu W, Zhou Q, Gu S, Wang Z, Xing B (2020) Size matters: Nano-biochar triggers decomposition and transformation inhibition of antibiotic resistance genes in aqueous environments. Environ Sci Technol 54:8821-8829

Liang, Y., Wang, G., Li, X., Zhang, Q., Zhan, H., Bi, S., and Liu, W. (2022). In situ preparation of a ferric polymeric aluminum chloride–silica gel nanocatalyst by mechanical grinding and its solid-phase catalytic behavior in organic synthesis. *New Journal of Chemistry*, *46*(31), 15110-15117.

Luo Y, Wang Y, Zhu Y, Xue M, Zheng A, Han Y, Yin Z, Hong Z, Xie C, Li X, Lei S, Gao B (2022) Ball-milled bismuth oxychloride/biochar nanocomposites with rich oxygen vacancies for reactive red-120 adsorption in aqueous solution. Biochar 4:21

Lyu H, Gao B, He F, Zimmerman AR, Ding C, Huang H, Tang J (2018) Effects of ball milling on the physicochemical and sorptive properties of biochar: Experimental observations and governing mechanisms. Environ Pollut 233:54-63

Mei, H., Huang, W., Wang, Y., Xu, T., Zhao, L., Zhang, D., ... and Pan, X. (2022). One stone two birds: Bone char as a cost-effective material for stabilizing multiple heavy metals in soil and promoting crop growth. *Science of The Total Environment*, *840*, 156163.

Naghdi M, Taheran M, Brar SK, Kermanshahi-pour A, Verma M, Surampalli RY (2017) Immobilized laccase on oxygen functionalized nanobiochars through mineral acids treatment for removal of carbamazepine. Sci Total Environ 584:393-401

Park JH, Wang JJ, Zhou B, Mikhael JER, DeLaune RD (2019) Removing mercury from aqueous solution using sulfurized biochar and associated mechanisms. Environ Pollut 244:627-635

Pratap T, Chaubey AK, Patel M, Mlsna TE, Pittman CU Jr, Mohan D (2022) Nanobiochar for aqueous contaminant removal. In: Mohan D, Pittman CU, Mlsna TE (eds) Sustainable biochar for water and wastewater treatment. Elsevier, Amsterdam, pp 667-704

Qu, J., Tian, X., Jiang, Z., Cao, B., Akindolie, M. S., Hu, Q., and Zhang, Y. (2020). Multi-component adsorption of Pb (II), Cd (II) and Ni (II) onto microwave-functionalized cellulose: Kinetics, isotherms, thermodynamics, mechanisms and application for electroplating wastewater purification. *Journal of hazardous materials*, *387*, 121718.

Ramanayaka S, Tsang DCW, Hou D, Ok YS, Vithanage M (2020a) Green synthesis of graphitic nanobiochar for the removal of emerging contaminants in aqueous media. Sci Total Environ 706:135725

Ramanayaka S, Vithanage M, Alessi DS, Liu WJ, Jayasundera ACA, Ok YS (2020b) Nanobiochar: Production, properties, and multifunctional applications. Environ Sci Nano 7:3279-3302

Ren SY, Xu X, Hu KS, Tian WJ, Duan XG, Yi JB, Wang SB (2022) Structure-oriented conversions of plastics to carbon nanomaterials. Carbon Res 1:15

Shamsollahi, Z., and Partovinia, A. (2019). Recent advances on pollutants removal by rice husk as a bio-based adsorbent: A critical review. *Journal of environmental management*, *246*, 314-323.

Shang, Y., Hasan, M. K., Ahammed, G. J., Li, M., Yin, H., & Zhou, J. (2019). Applications of nanotechnology in plant growth and crop protection: a review. *Molecules*, *24*(14), 2558.

Singh R., Srivastava P., Singh P., Sharma A.K., Singh H., Raghubanshi A.S. (2019). Impact of rice-husk ash on the soil biophysical and agronomic parameters of wheat crop under a dry tropical ecosystem. Ecol Indic 105:505-515

Singh, V.; Pant, N.; Sharma, R.K.; Padalia, D.; Rawat, P.S.; Goswami, R.; Singh, P.; Kumar, A.; Bhandari, P.; Tabish, A.; and Deifalla A. M. (2023). Adsorption Studies of Pb(II) and Cd(II) Heavy Metal Ions from Aqueous Solutions Using a Magnetic Biochar Composite Material. Separations 2023, 10, 389.

Sun Y, Lyu H, Cheng Z, Wang Y, Tang J (2022) Insight into the mechanisms of ball-milled biochar addition on soil tetracycline

degradation enhancement: Physicochemical properties and microbial community structure. Chemosphere 291:132691

Syafalni, S., Sing, S., Zawawi, M. (2014). Sorption of dye wastewater by using natural zeolite, anionic-cationic surfactant modified zeolite and cationic surfactant modified zeolite. World Appl. Sci. J. 32, 818–824.

Tahoon M. A., Siddeeg S. M., Alsaiari N. S., Mnif W., and Ben Rebah F. (2020). Heavy Metals Removal from Water Using Nanomaterials: A Review. *Processes* 2020, 8, 645; doi:10.3390/pr8060645

Tan, X. F., Zhu, S. S., Wang, R. P., Chen, Y. D., Show, P. L., Zhang, F. F., & Ho, S. H. (2021). Role of biochar surface characteristics in the adsorption of aromatic compounds: Pore structure and functional groups. *Chinese Chemical Letters*, *32*(10), 2939-2946.

Temkin, M., & Pyzhev, V. (1940). Kinetics of ammonia synthesis on promoted iron catalyst. Acta Physicochimica, USSR, 12, 327-356.

Trakal L, Bingöl D, Pohorˇely M, Hruška M, Komárek M (2014) Geochemical and spectroscopic investigations of Cd and Pb sorption mechanisms on contrasting biochars: engineering implications. Bioresour Technol 171:442–451. https://doi.org/10.1016/j.biortech. 2014.08.108

Tran, H. N. (2022). Improper estimation of thermodynamic parameters in adsorption studies with distribution coefficient KD (qe/Ce) or Freundlich constant (KF): considerations from the derivation of dimensionless thermodynamic equilibrium constant and suggestions. *Adsorption Science & Technology*, *2022*.

Vishnu D, Dhandapani B, Vaishnavi G, Preethi V (2022) Synthesis of tri-metallic surface engineered nanobiochar from cynodon dactylon residues in a single step-batch and column studies for the removal of copper and lead ions. Chemosphere 286:131572

Wang K, Sun Y, Tang J, He J, Sun H (2020) Aqueous Cr(VI) removal by a novel ball milled Fe0-biochar composite: Role of biochar electron transfer capacity under high pyrolysis temperature. Chemosphere 241:125044

Wang Y, Wang L, Li Z, Yang D, Xu J, Liu X (2021) MgO-laden biochar enhances the immobilization of Cd/Pb in aqueous solution and contaminated soil. Biochar 3:175-188

Yin, M., Bai, X., Wu, D., Li, F., Jiang, K., Ma, N., ... and Fang, L. (2022). Sulfur-functional group tunning on biochar through sodium thiosulfate modified molten salt process for efficient heavy metal adsorption. *Chemical Engineering Journal*, *433*, 134441.

Younas F., Bibi I., Zulfqar A., Shahid M., Shakoor M. B., Hussain M. M., Niazi N. K., and Nawaz M. F. (2023). Environmental Applications of Natural and Surface-Modified Zeolite. In: M. Vithanage et al. (eds.), *Clay Composites*, Springer Nature Singapore Pte Ltd, pp. 373-396. https://doi.org/10.1007/978-981-99-2544-5_17

Younes A.A., Abdulhady Y.A.M., Shahat N.S. and El-Din El-Dars F.M.S. (2019). Removal of cadmium ions from wastewaters using corn cobs supporting nano-zero valent iron, Separation Science and Technology, DOI: 10.1080/01496395.2019.1708109

Yue Y, Shen C, Ge Y (2019) Biochar accelerates the removal of tetracyclines and their intermediates by altering soil properties. J Hazard Mater 380:120821

Zama E.F., Reid B.J., Arp H.P.H., Sun G.X., Yuan H.Y., Zhu Y.G. (2018). Advances in research on the use of biochar in soil for remediation: a review. J Soils Sed 18:2433-2450

Zeng Z, Ye S, Wu H, Xiao R, Zeng G, Liang J, Zhang C, Yu J, Fang Y, Song B (2019) Research on the sustainable efficacy of g-MoS decorated biochar nanocomposites for removing tetracycline hydrochloride from antibiotic-polluted aqueous solution. Sci Total Environ 648:206-217

Zhang J, Hu X, Zhang K, Xue Y (2019) Desorption of calcium-rich crayish shell biochar for the removal of lead from aqueous solutions. J Colloid Interface Sci 554:417-423

Zhang X, Wells M, Niazi N, Bolan N, Shaheeng S, Hou D, Gao B, Wang H, Rinklebe J, Wang Z (2022) Nanobiochar-rhizosphere interactions: Implications for the remediation of heavy-metal contaminated soils. Environ Pollut 299:118810

تأثير المواد النانوية المشعة أو غير المشعة على معالجة المياه الملوثة بالرصاص والكادميوم

[2]ابراهيم عبد النبى ابراهيم شهاب. [1]أ.د/ هيثم محمد شحاته سالم,[2]أ.د/سليمان محمد سليمان , [2]أ.د/ يحيى جلال محمد جلال و[1]أ.د/ محمد على عبد السلام
[1]قسم الأراضى، والمياه كلية الزراعة، مشتهر، جامعة بنها.
[2] **قسم** بحوث الأراضى والمياه،مركز البحوث النووية ،هيئة الطاقة الذرية أبوزعبل 13759 –مصر .

تم تحضير الزيوليت النانوي المركب كيميائيا وفحم قش الأرز النانوي لاستخدامهما كممتزات للمياه الملوثة صناعيا بالرصاص والكادميوم. تم تحديد الخصائص والتكوين للجسيمات النانوية. تم استخدام حيود الأشعة السينية (XRD) والتحليل الطيفي بالأشعة تحت الحمراء (FT–IR)لتحديد المجموعات الوظيفية المسؤولة عن امتصاص ملوثات العناصر بواسطة الجسيمات النانوية .تم تحديد مجموعة الهيدروكسيل على أنها الذروة المكتشفة في تحليل FT–IR لزيوليت النانو ، في حين نسبت نطاقات شار قش الأرز إلى العديد من مجموعات الذروة الوظيفية الواسعة ، بما في ذلك مجموعات الهيدروكسيل وغيرها. تم التحقيق في أنشطة هذه الجسيمات النانوية عند قيم مختلفة لكتلة المواد الماصة النانوية ودرجة الحرارة. زيادة كتلة المواد الماصة النانوية من 0.25 إلى 0.75 جم ، وادى الى تحسن كبير في كفاءة إزالة العناصر قيد الدراسة. وبعد ذلك ، لم يغير 0.75 جم من كتلة الممتز الحيوي النانوي بشكل كبير عملية الامتصاص. بالنظر إلى أن ارتفاع درجة الحرارة يحسن التفاعل بين المادة الماصة وأيونات المعادن ، كشفت النتائج أن الحركة العالية لأيونات المعادن قد تكون مسؤولة أيضا عن زيادة امتصاص أيونات المعادن بواسطة مادة النانو الماصة. وعلاوة على ذلك، وبالمقارنة مع المواد الماصة غير المشعة، أظهرت المواد المشعة قدرة منخفضة على إزالة الرصاص والكادم. تشير قيم معامل الارتباط (R2) لكل من أيونات Pb (II) و Cd (II) إلى أن نموذج Langmuir نجح في وصف امتصاص كل من Cdو Pb مما يشير إلى أن الامتزاز هو العملية الرئيسية المسؤولة عن امتصاص Pb و Cd بواسطة المواد الماصة النانوية قيد الدراسة. تم تحديد قيم سعة الامتزاز القصوى (qmax) لأيونات Pb (II) و Cd (II) لتكون 4.09 مجم / جم و 7.18 مجم / جم ، على التوالي ، بناء على نموذج Langmuir.أشارت هذه النتائج إلى أنه بسبب المواقع النشطة ، كانت قيم الثابت K2 للمواد الممتزة الحيوية المعرضة لإشعاع جاما أكبر من القيم المقابلة للمواد الماصة النانوية غير المشعة.